

Electrochemical Studies on AB₅ Metal Hydrides

B. V. Ratnakumar, S. Surampudi, S. Di Stefano and G. Halpert
Jet Propulsion Laboratory, California Institute of Technology
4800, Oak Grove Dr., Pasadena, California 91109

Introduction

The ability of certain intermetallic alloys to reversibly absorb significant amounts of hydrogen at low pressures and high potentials is being exploited for several applications. In particular, the replacement of Cd in a Ni-Cd cell with the metal hydride (MH) anodes has resulted in substantial gains in the specific energy, energy density, cycle life and in the environmental compatibility. Also, the Ni-MH cells have the advantages of sustaining high discharge rates, fast charge rates and gas recombination processes during overcharge and overdischarge similar to Ni-Cd. With the voltage and the charge methods also being almost identical, the Ni-MH cells are expected to gain prominence over Ni-Cd in applications ranging from portable electronic appliances to electric vehicle.

Two classes of metal hydrides alloys based on rare earth metal (AB₅)^(1,2) and titanium (AB₂)⁽³⁾ are being currently developed at various laboratories. The AB₅ alloys are essentially based on LaNi₅ with various substituents for La as well as Ni to stabilize the alloy during charge-discharge cycling, by reducing the internal stress on hydrogen absorption and/or forming protective surface films. For example, the volume expansion is reduced by a partial substitution of Ni with Co and the interracial properties improved with small amounts of Al or Si⁽⁴⁾. Sakai et al⁽⁴⁾ studied the ternary alloys with different ternary solutes including Mn, Cr, Al, Co and Cu. The cycle life improves upon the substitution of Ni with the ternary solute in the order Mn < Ni < Cu < Cr < Al < Co. A substitution of the rare earth metal site with Ti⁽⁵⁾, Zr⁽⁶⁾, or other lanthanides such as Nd⁽¹⁾ and Ce⁽⁷⁾ render the formation of a protective surface film and enhance the cycle life. This eventually led to the use of relatively inexpensive misch metal, Mm, a naturally occurring mixture of rare earth metals (mainly La, Ce, Pr and Nd) in place of La. The use of misch metal also improved the durability of the alloy, as evident from the long cycle as well as the quantitative estimates of the surface layers (La(OH)₃ and Mm(OH)₃) on the cycled electrodes⁽²⁾. The alloy formulations currently in use thus contain (Mm)(Ni-Co-Mn-Al)₅^(8,9), often with other transition metal additives, such as W and Mo.

1 Despite the fact that the effect of the substitution of La with Ce and Nd were studied independently, the optimum composition of the misch metal has not been reported. Nor

are the effects of the La substituents on the electrochemical characteristics of the alloy understood. In this work, a systematic study has been attempted to vary the misch metal composition, especially with respect to the ratio of La and Ce, and to correlate their electrochemical behavior with their performance in alkaline rechargeable cells.

Experimental

These alloys were supplied by Rhone-Poulenc Basic Chemical Co.. Out of the several alloys supplied, representative samples were chosen that would vary essentially in the misch metal composition (Table I), with the transition metal composition (Ni sites) being approximately similar.

The as supplied alloys were pulverized by ball milling and/or hydrogen absorption-resorption cycles. The MH powder (< 75 μ) was mixed with 20 w% Ni powder (INCO type 255, -1 μ). Electrodes (1" x 1", -250 mAh) were made from the mixture of MH and Ni powders and 5 w% Teflon, by hot-pressing onto a Ni Exmet. Electrodes for the basic electrochemical studies were prepared by filling the cylindrical cavity in the BAS disk electrodes with the mixture of electrode powders and Teflon, of equal quantities in each case. This would ensure surface area, charge density (mAh/cm³) and porosity, thus permitting a comparison of different electrochemical parameters of the MH alloys. NiOOH electrodes from an aerospace Ni-Cd cell formed the counter electrode and a Hg/HgO served as the reference electrode. A three-electrode flooded cell with a Luggin capillary for the reference electrode was adopted for the basic electrochemical studies. A prismatic glass cell with nylon (Pellon) separator was employed for the cycle life studies. The electrolyte contained 31 w% KOH solution. Electrochemical experiments were performed with 273 EG&G Potentiostat/Galvanostat interfaced with an IBM-PC. Cycling of the cells was carried out with an in-house automatic battery cycler at constant current (4 mA/cm², C/5 rate) to -0.5 V vs. Hg/HgO during discharge and to charge return of 120%.

Results and Discussion

Cyclic Voltammetry : Cyclic voltammetry was carried out in the anodic range from the open circuit potential (-0.6 V vs. Hg/HgO) to 0.4 V vs. Hg/HgO on the virgin alloy, i.e.,

before incorporating any hydrogen therein. This is expected to provide a comparative assessment of the susceptibility of the alloys towards oxidation. The oxidation of the MH alloy forming a passive surface film is one of the prominent modes of failure of the MH electrodes during charge-discharge cycling⁽³⁾. Such an oxidation is also responsible for a reduced cycle life in oxygenated environments during overcharge, though the MH alloy is expected to be cathodically protected from oxidation. Also, the voltammetric studies in the above window are relevant to the practical application i.e., during deep discharge, especially when the MH becomes capacity-limiting.

The DC cyclic voltammetric curves of the MH electrodes revealed no peaks corresponding to the oxidation of the major alloying elements, e.g., La, Ce, Ni, Co and Mn. This is not surprising, since the reversible potentials of all the alloying elements (La: -2.9, Ce: -2.87, Co: -0.73 V, Mn: -1.55 V and Ni: -0.72 V vs. Hg/HgO) are negative to the open circuit potential, such that they would exist only in the oxidized form, as evident from the AES studies on the alloy surfaces⁽³⁾. A deoxygenation of the electrolyte hasn't altered the voltammograms, implying that the peaks are related to the hydroxyl ions instead to dissolved oxygen. All the MH alloys exhibited strong peak @ 0.4 V, which may be attributed to the oxygen evolution. Also, its conjugate reduction peak was also observed in the reverse scan. This points to a possibility of using the MH electrode as the current collector for the oxygen reaction in alkaline media, which may be exploited in the fields of rechargeable metal-air cells or fuel cells.

Charge Discharge Behavior

Galvanostatic cathodic (charge) and anodic (discharge) polarization curves were obtained at 17 and 57 mA/cm², respectively. The electrodes were overcharged -400 mAh/g to ensure complete hydriding of the MH alloy. The anodic polarization (discharge) curves (Fig. 1) reveal that the discharge voltages decrease in the order 6025 > 6077 or 6026 > 6039 > IBA 5. The discharge specific capacity obtained under these conditions increases in the order LaNi₅ < IBA 5 < 6039 < 6026 < 6025 (Fig. 7). This may be a result of incomplete charging of some of the alloys due to their high (> 1 atm) equilibrium pressure.

Electrochemical Isotherms

Electrochemical isotherms were generated for the MH alloys from the equilibrium electrode potentials at various concentration of hydrogen in the alloy (state of charge), after effecting absorption / desorption of known quantities of hydrogen by constant current charging and discharging,

respectively. The equilibrium electrode potentials are related to the equilibrium hydrogen pressure, P_{H₂} as

$$E_{o(\text{vs. HgO/Hg})} = -0.9324 - 0.0291 \ln(P_{H_2})$$

The electrochemical (EC) isotherms during absorption (Fig. 2) are slightly different from the gas phase isotherms, i.e., the inflection in the pressure at the end of absorption is absent, possibly due to the cell internal pressures limited by the present design. The discharge isotherms, on the other hand are much similar to the gas phase isotherms. The absorption equilibrium pressure for the MH alloy decrease in the order 5978 (300 psig) > 6039 (60) > 6077 (40) > 6026, which is the same order for the variation of the specific discharge capacity. Apparently, the equilibrium pressure reflects the chargeability of the alloy under the present conditions. The discharge isotherms reveal the ease of oxidation of the alloys. The desorption equilibrium pressure is to be higher than 10³ to facilitate desorption.

DC Polarization Studies

Often, the kinetics of hydrogen absorption / desorption are slowed down by the addition of (film-forming) substituents added to stabilize the alloy. In order to determine the effects of the substitution of La with Mm (especially Ce) on the discharge / charge kinetics, DC polarization experiments were carried out on the alloys and kinetic parameters were evaluated therefrom. Micropolarization and Tafel experiments were conducted separately on the alloys under potentiodynamic conditions at scan rates of 0.02 mV/s and 0.5 mV/s, respectively. The scan rates were so chosen as to provide near-steady state conditions and yet with minimal changes in the electrode state of charge or surface conditions.

The values of polarization resistance estimated from the slopes of micropolarization curves of different MH alloys (Fig. 3) are fairly identical with a marginal decrease in the order 5978 > 6025 > IBA 5 > 6077 > 6026 > 6039. The Tafel polarization curves (Fig. 4) also seem to be identical for different MH alloys, except for slight differences. The polarization curves were obtained from the anodic segment, to avoid potential fluctuations due to the hydrogen evolved on the electrode during reduction. The curves indicate strong mass transfer effects at high currents. From the Tafel plots, the overpotentials at any cd. increase in the order 6039 > 6026 (6077) > 5978 > IBA 5 > 6025. The exchange current densities from the Tafel plots are of the order 10⁻³-10⁻² A/cm² and the transfer coefficients are 0.12-0.23. The cathodic Tafel segments often show two distinct slopes (e.g., LaNi₅), due to the occurrence of hydrogen evolution reaction.

Cycle Life Studies

Finally, the performance of the **MH** alloys during charge-discharge cycling was evaluated in 250 mAh, negative limited, prismatic, laboratory test cells. Despite the fact that the seated cells are typically made in the positive - limited mode to permit overcharge mechanism, the present cells were designed to understand the life-limiting mechanisms at the MH electrode. These cells were overcharged by 120% to ensure complete charging. Accordingly, the cycle lives under these conditions are expected to be shorter than in the scaled configuration.

The cycle life of the cells containing different **MH** alloys are reported in Fig. 5. As may be expected there is a wide range in the cycle life; the shortest being for LaNi_5 that has poor chargeability and increases in the order 6039 < IBA 5 < 6077 < 6026 or 6025. In the course of the cycling the end of charge voltage shows a gradual increase, the voltage decreasing once again in the above order.

Effect of Misch Metal Composition

The above cycling studies may be recast as in Fig. 6, to illustrate the effect of the **misch** metal composition on the cycle life. As may be seen from the figure, the cycle life improves upon substituting La with Ce, and tends to level off around 30 mol % La and 50 mol% Ce. The initial capacity also seem to improve with an increase in a similar manner ratio. The kinetics of the **hydriding** are relatively unaffected by the substitution of La with Ce. The optimum composition for the **misch** metal in the MH alloy would thus contain around 30 mol % of La and 50 mol % of Ce with the remainder being Nd and Pr.

Conclusions

Various electrochemical studies carried out on the **MH** alloys revealed that the optimum composition for the **misch** metal in the AB_5 should contain a% of Ce (and % of Nd and Pr) in place of La to decrease the equilibrium pressure, improve the charge ability, and enhance the cycle life with no ill-effects on the kinetics. The **MH** alloy electrodes facilitate electrochemical reduction or evolution of oxygen which may be exploited in the fields of metal-air cells and fuel cells.

Acknowledgments

The work described here was carried out at the Jet Propulsion Laboratory, California Institute of Technology, under contract with the National Aeronautics and Space Administration, This program is sponsored by the Office of

Advanced Concepts and Technology. Gratitude is extended to Dr. Bao-Min Ma of Rhone Poulenc Basic Chemical Co., for providing the **MH** alloys.

References

1. J. G. G. Willems, *Philips J. Res.*, 39 (Suppl. 1), 1 (1984); J. J. G. Willems and K. H. J. Buschow, *J. Less Common Metals*, 129, 13 (1987).
2. T. Sakai, K. Muta, H. Miyamura, N. Kuriyama and H. Ishikawa, *Proc. Symp. Hydrogen Storage Materials: Batteries and Electrochemistry*, ECS Proc. Vol. 92.-5, p. 59 (1992); T. Sakai, H. Yoshinaga, H. Miyamura and H. Ishikawa, *J. Alloys and Compounds*, 180,37 (1992).
3. S. R. Ovshinsky, M. A. Fetcenko and J. Ross, *Science*, 260, 176 (1993); M. A. Fetcenko, S. Venkatesan and S. R. Ovshinsky, *Proc. Symp. Hydrogen Storage Materials: Batteries and Electrochemistry*, ECS Proc. Vol. 92-5, p. 141 (1992). M. A. Fetcenko, S. Venkatesan, K. C. Hong and B. Reichman, *Power Sources*, Vol. 12, p. 411 (1988).
4. T. Sakai, K. Oguru, H. Miyamura, N. Kuriyama, A. Kato and H. Ishikawa, *J. Less-Common Metals*, 161, 193 (1990).
5. T. Sakai, H. Miyamura, N. Kuriyama, A. Kato, K. Oguru and H. Ishikawa, *J. Less-Common Metals*, 159, 127 (1990).
6. T. Sakai, H. Miyamura, N. Kuriyama, A. Kato, K. Oguru and H. Ishikawa, *J. Electrochem. Soc.*, 137, 795 (1990).
7. T. Sakai, T. Hazama, H. Miyamura, N. Kuriyama, A. Kato and H. Ishikawa, *J. Less-Common Metals*, 172-174, 1175 (1991).
8. N. Furukawa et al (Sanyo Electric Co.), *Proc. IBA Meeting, Seattle, WA, OCT. 12-13* (1990).
9. L. Matsumoto and A. Ohta, *Proc. IBA Meeting, Seattle, WA, OCT. 12-13* (1990).

Table -1: Composition of Rhone - Poulenc AB_5 MH Alloys

COMPOSITION (mol %)								
ALLOY #	La	Ce	Nd	Pr	Ni	Co	Mn	Al
5978	1	0	0	0	4.96	0	0	0
6025	0.3	0.51	0.07	0.13	3.56	0.76	0.4	0.3
6026	0.25	0.55	0.07	0.13	3.68	0.75	0.4	0.34
6039	0.64	0.25	0.04	0.08	3.51	0.77	0.4	0.31
6077	0.49	0.2	0.09	0.22	3.05	1.5	0	0.53

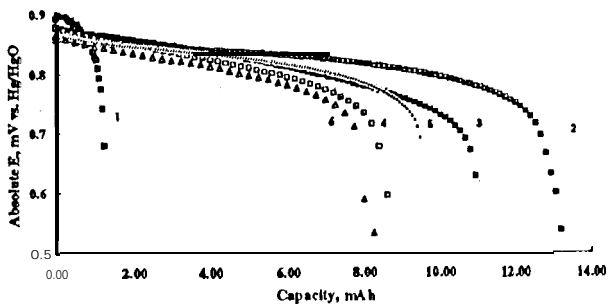


Fig. 1: Discharge curves of 1) 5978, 2) 602S, 3) 6026, 4) 6039, 5) 6077 and 6) IBA 5 MH alloy disc electrodes in flooded glass cell.

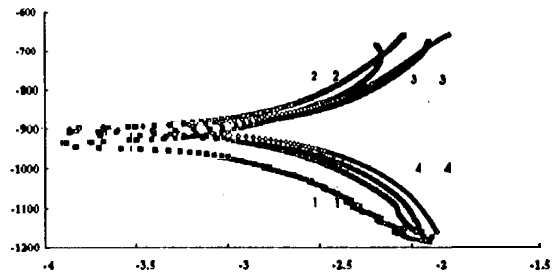


Fig. 4: Tafel polarization curves of 1) 5978, 2) 6025, 3) 6026 and 4) 6039 MH alloys.

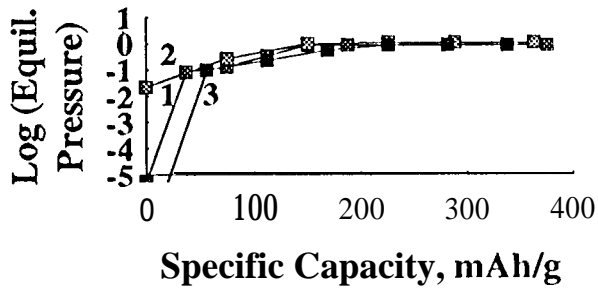


Fig. 2: Electrochemical isotherms of 1) 6077, 2) 6039 and 3) 6026 MH alloys during hydrogen absorption (reduction).

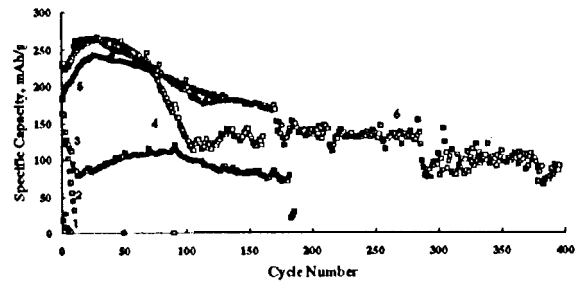


Fig. 5: Cycle life curves of 1) 5978, 2) 6039, 3) IBA 5, 4) 6077, 5) 6026 and 6) 6025 MH alloys in ~250 mAh, negative-limited cells @ C/5 charge and discharge.

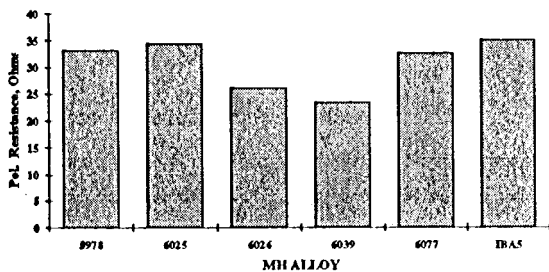


Fig. 3: Polarization resistances of MH alloys estimated from DC micropolarization experiments.

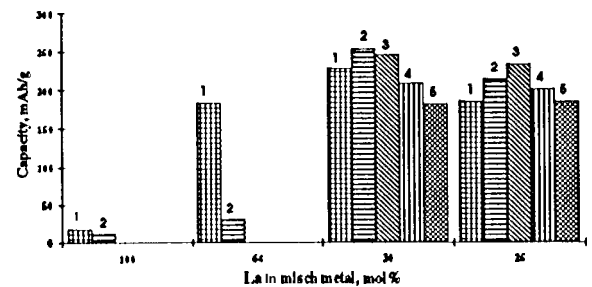


Fig. 6: Illustration of the dependence of capacity retention during charge-discharge cycling, on the misch metal composition.